LAWRENCE
LIVERMORE
NATIONAL
LABORATORY

UCRL-JRNL-205887

First Demonstration of a Meter-Scale Multilayer Dielectric Reflection Grating for High-Energy Petawatt-Class Lasers

J. A. Britten, H. T. Nguyen, L. M.JonesII, T. C. Carlson, C. R.Hoaglan, L.J. Summers, M. D. Aasen, A. Rigatti, and J. Oliver

July 20, 2004

Optics Letters

This document was prepared as an account of work sponsored by an agency of the United States Government. Neither the United States Government nor the University of California nor any of their employees, makes any warranty, express or implied, or assumes any legal liability or responsibility for the accuracy, completeness, or usefulness of any information, apparatus, product, or process disclosed, or represents that its use would not infringe privately owned rights. Reference herein to any specific commercial product, process, or service by trade name, trademark, manufacturer, or otherwise, does not necessarily constitute or imply its endorsement, recommendation, or favoring by the United States Government or the University of California. The views and opinions of authors expressed herein do not necessarily state or reflect those of the United States Government or the University of California, and shall not be used for advertising or product endorsement purposes.

First demonstration of a meter-scale multilayer dielectric reflection grating for high-energy Petawatt-class Lasers

J. A. Britten, H.T. Nguyen, L.M. Jones II, T.C. Carlson, C.R. Hoaglan, L.J. Summers, M.D. Aasen, J.D. Nissen

Lawrence Livermore National Laboratory, Livermore, CA 94550

A. Rigatti, and J. Oliver

Univ. Rochester Laboratory for Laser Energetics, Rochester, NY 14623

Abstract

We report on the design, fabrication and characterization of multilayer dielectric diffraction gratings of 800 x 400 rectangular aperture, suitable as pulse-compression optics for high-energy Petawatt-class laser systems. These gratings are approximately 2 times the size of any high-efficiency dielectric reflection grating previously reported. They exhibit quarter-wave diffracted wavefront at use wavelength and angle, and have uniform, high efficiency across the entire aperture.

Copyright

OCIS codes 050.1950, 090.2880, 140.7300, 220.4610, 310.1620, 320.5520

The design and construction of a new generation of high-energy Petawatt-class laser systems is currently proceeding at a number of institutions around the world[1-4]. These lasers require large-aperture diffraction gratings to compress amplified, temporally-stretched pulses using the technique of chirped-pulse amplification[5]. The potential for increased energy and power handling capacity of multilayer dielectric (MLD) gratings make them the optic of choice for

these new lasers, supplanting the gold-overcoated photoresist gratings used in the world's first Petawatt laser at LLNL[6] and currently in use elsewhere[7,8]. MLD gratings have been in existence since the mid 1990's[9] . They are considerably more complex to manufacture compared with gold-overcoated gratings. Only very recently have ~400 mm aperture MLD gratings been reported[10,11]. Gratings at this size are still too small to use at the energy levels and incidence angles planned. Development is underway to create the required apertures by coherent addition of up to three individual gratings in a linear array [12]. Due to the complexity of phasing discrete grating apertures to the degree of precision required, it is of great interest to increase the size of pulse compression gratings. We report here on the first demonstration of 800 x 400 mm MLD gratings meeting the specifications required by the laser builders.

The optical design of a high-efficiency MLD grating is subject to a number of constraints related to its manufacturability[13] . We choose to design a dichroic multilayer coating that is highly reflective at the use angle and wavelength, and minimally reflective at the holographic exposure angle and wavelength. This is to minimize 'reflective notching' common to pattern generation in photoresist on reflective structures, that impacts linewidth control. The second criterion in particular places demands on the accuracy of the coating deposition. We could choose to deposit a simpler quarter-wave design and use a sacrificial absorptive coating between the multilayer stack and the photoresist film, but this increases complexity and risk for other aspects of the grating manufacturing process, particularly at large apertures. The design must also be insensitive to coating deposition and grating linewidth variations that can be expected to occur over the apertures considered here.

The grating can be etched into one or several of the deposited dielectric layers. We choose to have a single thick SiO_2 layer comprising the grating due to the intrinsic high laser damage threshold of SiO_2. Directly underneath this grating layer we deposit an etch-stop layer consisting of an optical material that is resistant to our ion-beam etching process. This assures that the grating depth and its uniformity are determined by the deposition process, and relaxes the tolerances of subsequent manufacturing steps. In the case of these demonstration gratings, the high-and low index layers comprising the stack were made of HfO_2 and SiO_2, and the etch stop layer was Al_2O_3. The final design was the result of numerous iterations based on performance and deposition error-tolerance considerations.

Two large substrates were processed for this demonstration: an 800 mm diameter, 12 mm thick fused silica disk with chords cut on opposite sides to make a 400 mm short aperture; and a standard polarizer substrate for LLNL's National Ignition Facility laser, 807 x 417 x 90 mm, made of BK7 glass. The multilayer dielectric coating was deposited at the Univ. of Rochester Laboratory for Laser Energetics, using the reactive electron-beam evaporation process developed for production of NIF components[14]. Oxygen backfill during the SiO_2 deposition was adjusted to maintain compressive stress in a dry environment[15]. A number of smaller substrates were coated simultaneously for witnesses.

The multilayer-coated substrates were treated with a photoresist adhesion-promoter, coated with ~550 nm of photoresist using a meniscus coating process[16] , then baked in a convection oven overnight. The grating pattern was exposed into the photoresist layer using LLNL's large laser interference lithography station, utilizing 1.1 meter-diameter collimating lenses and 413 Kr-ion

laser light. After pattern development, the photoresist grating lines were examined at several locations using a custom large-bridge atomic force microscope capable of nondestructive measurement of submicron line widths anywhere on a 400 x 800 mm aperture. These measurements verified the uniformity of the exposure/development process. The optics were then hardbaked to increase the resistance of the photoresist grating mask to the ion-beam etching process.

The photoresist grating structure was transfer-etched into the top SiO2 layer of the grating using a custom reactive ion-beam etching (RIBE) tool[17] capable of etching submicron features into substrates as large as 2000 x 1000 mm. This utilizes a linear 1.1-meter commercial RF-generated ion beam configured for reactive etching using a gas mix of CHF_3, Ar and O_2, for increased selectivity of oxide-to-resist etch rate. The ion source is optimized for uniform beam current, and is mounted vertically in the center of a long vacuum chamber. The substrate passes back and forth laterally across the beam at a constant rate, removing a few nm of material per pass until the desired etch depth is attained. Figure 1 shows the resist-patterned 400x800 mm grating mounted in the etcher prior to RIBE.

After RIBE, the remaining photoresist mask was chemically stripped. The finished gratings were then subjected to full-aperture metrology including interferometry for diffracted and reflected wavefront, and photometry for the absolute efficiency in the -1 order. Witness parts processed from the same MLD coating batch as ride-alongs were cleaved and subjected to scanning electron microscopy.

The 80 cm diameter truncated fused silica disk was the first large grating processed. The -1 order diffraction efficiency at 1053 nm, 73.5^o incidence angle is shown in Figure 2. The uniformity of the diffraction efficiency to better than 1.2% RMS is a result of the etch-depth uniformity built into the design and the grating linewidth control exhibited by our process. An SEM of a ride-along grating is shown in Figure 3. Although atomic force microscopy cannot determine the details of the shape of the grating lines, the similarity of the AFM profiles of the ride-alongs and the full-sized part indicate that the grating profiles of the large part are nominally identical to those of the ride-alongs.

The second large grating, patterned on the NIF polarizer substrate, was examined by full-aperture phase-shifting interferometry at 1064 nm, both at ambient conditions and in a dry nitrogen-purged environment to simulate the wavefront alteration under use conditions in vacuum. Measurements were made at the Littrow condition (71.2^o @ 1064 nm) for both orientations: grating surface normal rotated CW (→/) and CCW (→\) with respect to the incoming beam. The zero-order reflected wavefront was also measured. Figure 4 shows the diffracted wavefront in the →\ orientation under dry conditions. The overall PV of 0.255 waves is considered to be extremely good for an optic of this size and shape that has both surface figure and holographic errors. Table 1 summarizes interferometric data of all of the measurements. The zero order wavefront and the →/ diffracted wavefront are dominated by convex astigmatism in the long axis. The convex cylinder error in the reflected wavefront is due to warping by residual compressive stress in the multilayer coating. It appears that in the →\ orientation astigmatism from holographic error largely cancels the coated surface figure error, while in the →/ orientation these errors add to worsen the diffracted wavefront. Of particular note is the very

minor change in wavefront exhibited between ambient and dry environments. This is atypical of standard MLD coatings manufactured by this process. Often, exposure to a dry environment causes water loss in porous e-beam evaporated coatings, resulting in the buildup of tensile stresses. In extreme cases the coating will crack or craze due to these stresses. The residual compressive stress of this coating, even after etching through the thick SiO_2 top layer and exposure to dry conditions, ensures that the coating will not craze under use conditions.

The diffraction efficiency of this grating at 1053nm, 73.5^o, and TE polarization is shown in Figure 5. It is about 4% lower than that of the first large grating above. However, the spatial uniformity is again very good. An SEM of a ride-along part for this run is shown in Figure 6. Comparison with Figure 3 shows that the grating profiles in this run are more vertical. This was done intentionally by modifying the ion beam parameters. The SEM also shows that the second layer of the multilayer stack has been partially etched away chemically during the resist stripping process. Figure 7 shows the calculated diffraction efficiency as a function of etched depth of this second layer. As can be seen, erosion of this layer has a significant effect on diffraction efficiency, and explains the lower efficiency of this part. We are working on design and process modifications that will eliminate this potential in future gratings.

This work was performed under the auspices of the United States Department of Energy by the Lawrence Livermore National Laboratory under contract no. W-7405-Eng-48.

References

1. C.P.J. Barty et.al, *Nuclear Fusion*, (in press), (2004)

2. N. Blanchot et. al., Proc. Intl. Fusion Sciences Applications Conf., Monterey, CA (2003)

3. D. Meyerhofer et. al., Proc. Intl. Fusion Sciences Applications Conf., Monterey, CA (2003)

4. R. Kodama et al, Plasma *Phys. Control. Fusion* **44**, B109 (2002).

5. D. Strickland and G. Mourou, *Opt. Commun*., **56**, 219, (1985)

6. M.D. Perry, D. Pennington, B.C. Stuart, G. Tietbohl, J.A. Britten, C. Brown, S. Herman, B. Golick, M. Kartz, J. Miller, H. T. Powell, M. Vergino, V. Yanovsky*, Opt*. *Lett*, **24**, 160, (1999)

7. Kitagawa, Y., Fujita, H. Kodama, R., Yoshida, H., Matsuo, S, Jitsuno, T., Kawasaki, T., Kitamura, H., Kanabe, T., Sakabe, S., Shigemori, K., Miyanaga, N., Izawa, Y., IEEE *J. Quant. Elect.,* **40,** 281, (2004)

8. M.H.R Hutchinson, D. Neely, B.E. Wyborn, Proc. SPIE V4424, 63, (2001).

9. M.D. Perry, R.D. Boyd, J.A. Britten, D. Decker, B.W. Shore, C. Shannon, E. Shults, and L. Li, *Opt. Lett.,* **20(8)** 940, (1995)

10. J.A. Britten, S.J. Bryan, L.J. Summers, H.T. Nguyen, B.W. Shore, O. Lyngnes. *Conference on Lasers and Electro-Optics. Conference Edition (IEEE Cat. No.02CH37337). Opt. Soc. America. V2, 2002, pp.CPDB7-1-4 vol.2. Washington, DC, USA*

11. B. Touzet and J.R. Gilchrist, *Phot. Spectra*, 68, Sept. 2003

12. T.J. Kessler, J. Bunkenburg, H. Huang, A. Kozlov, and D.D. Meyerhofer, *Opt. Lett.*, **29** 635, (2004)

13. B.W. Shore, M.D. Perry, J.A. Britten, R.D. Boyd, M.D. Feit, H. T. Nguyen, R. Chow, G. Loomis and L. Li, *JOSA A,* **14(5)**, 1124, (1997)

14. J.B. Oliver, J. Howe, A. Rigatti, D.J. Smith, and C. Stolz, OSA Technical Digest , Washington DC, 2001), ThD2 pp.1-3.

15. H. Leplan, B. Geenen, J.Y. Robic, and Y. Pauleau, *J. Appl. Phys*. **78,** 962, (1995).

16. J.A. Britten, *Chem. Eng. Comm.* **120** 59, (1993)

17. J.A. Britten, W. Molander, A.M. Komashko, C.P.J. Barty, Proc. SPIE V5273, 1, (2003)

Figure Captions

Figure 1. 400 x 800 mm grating loaded in reactive ion beam etcher.

Figure 2. -1 order diffraction efficiency at 1053 nm, 73.5^{o} incidence angle, and TE polarization, of 400 x 800 mm grating on 12 mm thick fused silica debris shield. Average=96.5%; RMS=1.2%of average, max = 99.2%. 10,000 data points.

Figure 3. Scanning electron micrograph of 50 mm witness grating from same coating batch processed as a ride-along with the grating of Figure 2.

Figure 4. A: Full-aperture diffracted wavefront of 400 x 800 x100 mm 1780 l./mm MLD grating at 1064 nm, 71.2^{o} incidence angle, measured in a dry N_2 environment.

Figure 5. -1 order diffraction efficiency at 1053 nm, 73.5^{o} incidence angle, TE polarization, of 1780 l/mm grating on 400 x 800 x 100 mm BK7 substrate. Average=92.0%; RMS=1.6% of average, max = 95.7%. 10,000 data points. 90% contours shown.

Figure 6. Scanning electron micrograph of 50 mm witness grating from same coating batch processed as a ride-along with the grating of Figure 4-6.

Figure 7. Plot of calculated diffraction efficiency @ 1053 nm, 73.5^{o} incidence, TE polarization, of this grating design as a function of etched depth of the second layer.

Table 1.

Interferometry results for 800 x 400 mm grating measured at 1064 nm, Littrow angle (71.2^{o}).

Data are for reflected and diffracted wavefront, measured in waves at 1064 nm. →/ and →\ represent orientation of the grating with respect to the incoming light.

	Ambient		Dry	
reflected/ diffracted wavefront	**P-V Waves @ 1064 nm**	**RMS Waves @ 1064**	**P-V Waves @ 1064 nm**	**RMS Waves @ 1064**
-1 order -->/*	0.654	0.121	0.706	0.151
-1 order -->\	0.276	0.039	0.255	0.045
0 order	0.261	0.063	--	--

*Dominated by convex astigmatism along long axis.

FIGURES

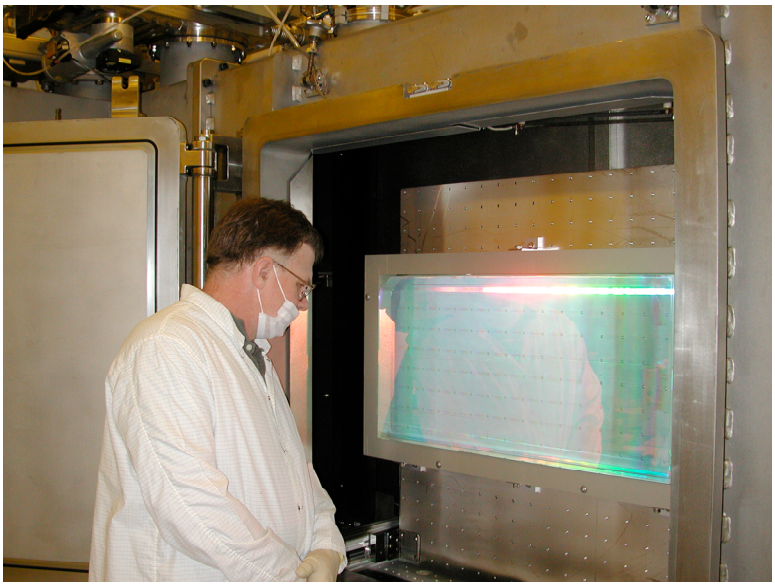

Figure 1

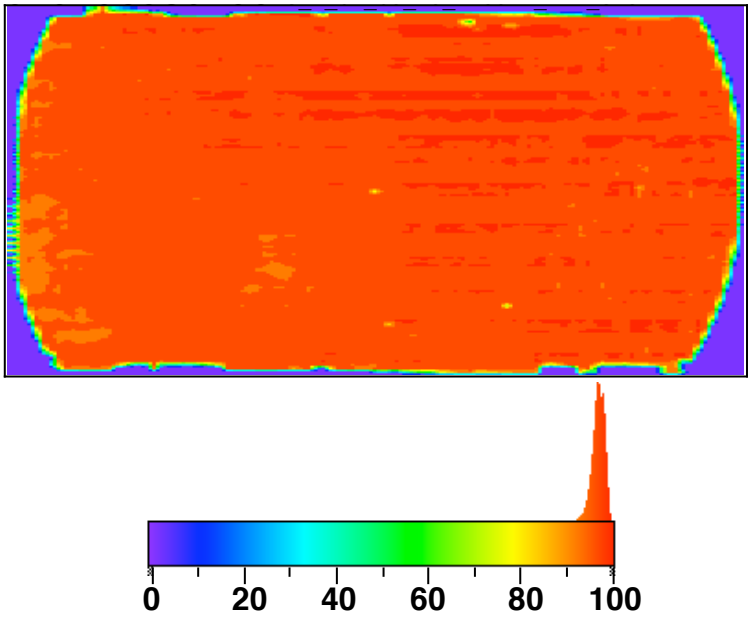

Figure 2.

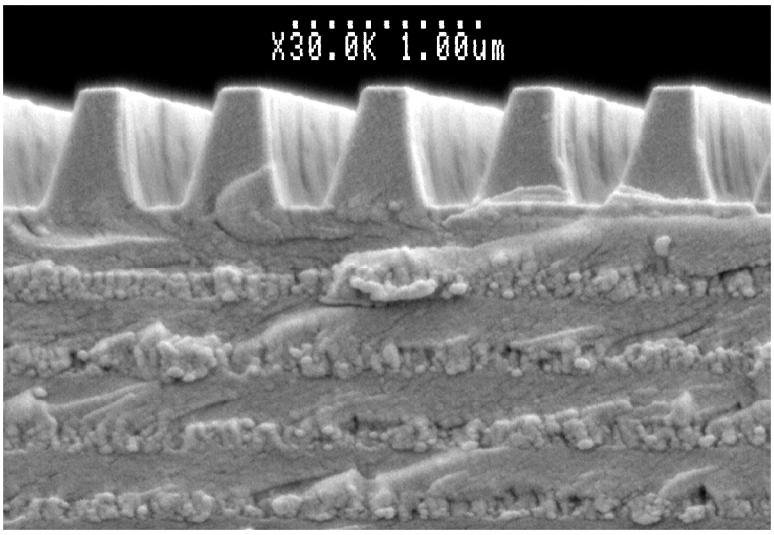

Figure 3.

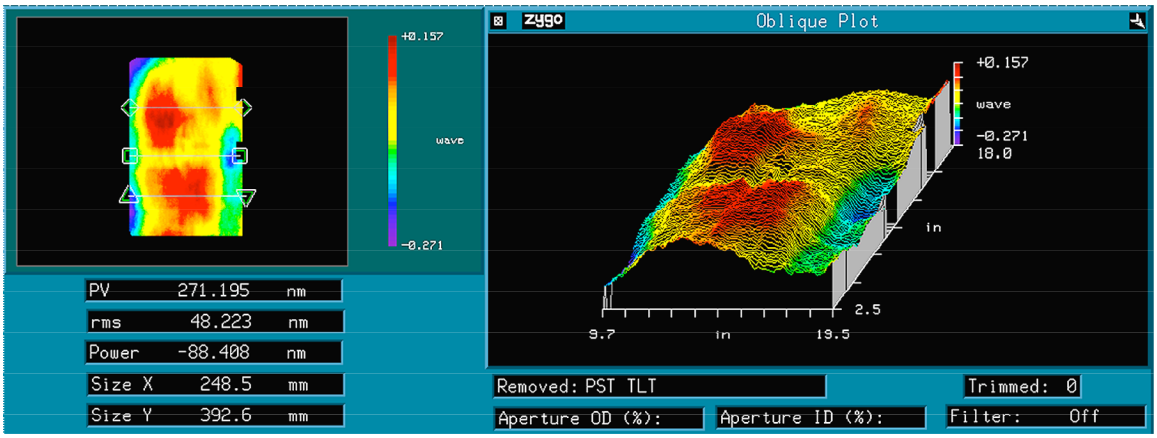
+0.157
wave
-0.271
PV 271.195 nm
rms 48.223 nm
Power -88.408 nm
Size X 248.5 mm
Size Y 392.6 mm
Zygo
Oblique Plot
+0.157
wave
-0.271
18.0
in
2.5
9.7
in
19.5
Removed: PST TLT
Trimmed: 0
Aperture OD (%):
Aperture ID (%):
Filter: Off

Figure 4

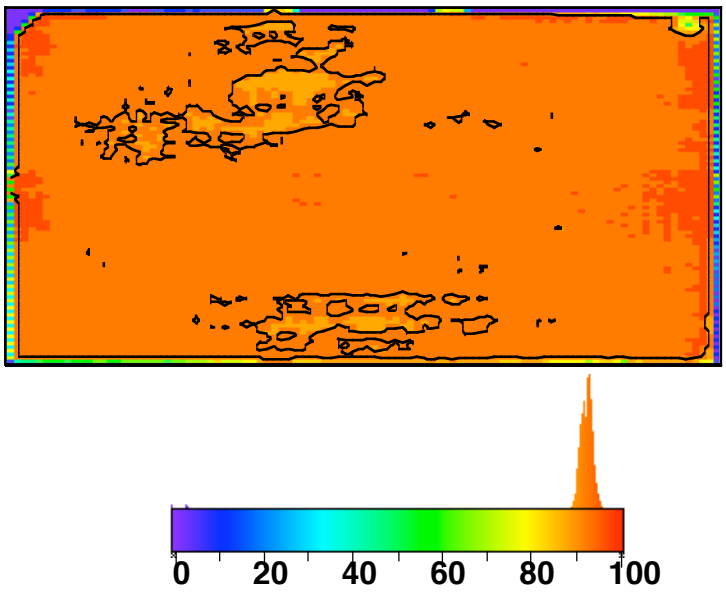

Figure 5

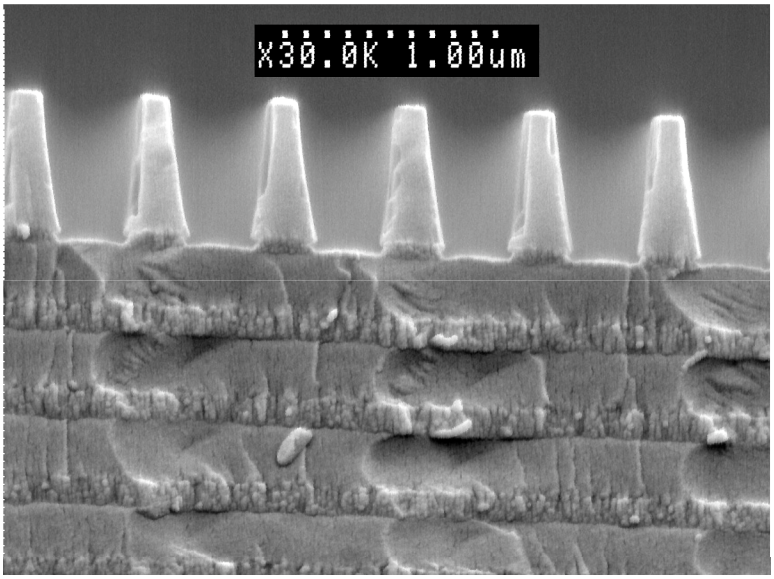

Figure 6

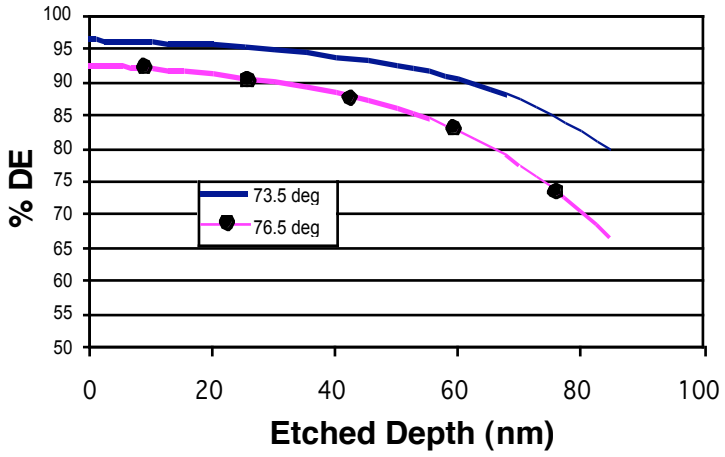
100
95
90
85
80
75
70
65
60
55
50
% DE
73.5 deg
76.5 deg
0
20
40
60
80
100
Etched Depth (nm)

Figure 7